JOURNAL OF MATERIALS SCIENCE 30 (1995) 628–632

Characterization of silver–palladium submicronic powders

Part I *Morphology and thermal properties*

E. DELARUE, M. MOSTAFAVI, M. O. DELCOURT*
Laboratoire de Physico-Chimie des Rayonnements associé au CNRS URA 75, Bat. 350, Université Paris-Sud, 91405 Orsay Cedex, France

D. REGNAULT
CLAL, 8 Rue Portefoin, 75003 Paris, France

Various properties of submicronic silver–palladium powders (70/30 and 75/25 Ag/Pd % wt/wt), recently obtained by a new process of precipitation in aqueous solution, are described. These powders are intended to be used in the multilayer ceramic capacitor industry. The morphology of the particles has been analysed through various measurements, such as SEM images, tap density, BET surface area, and the size distribution by a sedimentation technique. The powders were found to be made of spherical shaped particles of mean diameter close to 0.3 μm with a narrow size distribution. The individual grains were agglomerated only to a small extent. After being conditioned as a paste by blending with an organic binder, screen-printed and fired, the particles sintered into a conductive layer of low resistivity (15–30 μW cm for 2 μm thickness) with only a few remaining voids, as observed by SEM. Thermal measurements indicated no melting of a pure silver phase at 960 °C, thus indicating that alloying was achieved before this temperature.

1. Introduction

Intermetallic Ag–Pd powders are of increasing interest in the electronics and in multilayer ceramic chip capacitor (MLCC) industry where they are used as precursors of thin conductive films and termination inks [1–8]: they are preferred to pure silver powders because of their better thermal performances due to the high melting point of palladium (1550 °C compared to 960 °C for silver). A mixture of monometallic powders does not exhibit such performances because the silver particles begin to melt before the palladium ones.

With the aim to obtain thin, continuous and uniform metal films by the wet stack process, several points of interest concern the morphology of the powder particles. The process consists in dispersing the metal powder in an organic vehicle thus forming an ink, then screen-printing this ink on to an insulating substrate. Finally, the ensemble is fired in order to eliminate the organic binder and to allow the particles to sinter into a conducting layer. Homodisperse spherical shaped grains are the best adapted to compact planar arrangement with optimal contacts in view of sintering. The submicronic range for particle diameter is suitable in order to provide metal layers a few micrometres thick. A narrow particle size distribution is crucial for two reasons: first, large particles can perforate insulating layers, resulting in undesirable short-circuits; second, very tiny particles are known to catalyse the decomposition of the organic binder, resulting in delamination [1]. Furthermore, the dilatation and shrinkage of metal layers must match those of the dielectrics as close as possible.

The present paper deals with new bimetallic Ag–Pd powders recently synthesized at CLAL: the powders described here are made by co-precipitation of silver and palladium nitrates dissolved in water through the addition of a reductor. The powder is then centrifuged, carefully washed and dried under mild conditions. Some additives prevent the powder from agglomeration during the whole process. Many physical properties are presented concerning the powders in their original form, as well as after being fired into conductive films. These powders have been shown to be made of composite particles containing both metals in segregated domains: a silver core surrounded by a palladium layer [9].

*Author to whom all correspondence should be addressed.

0022–2461

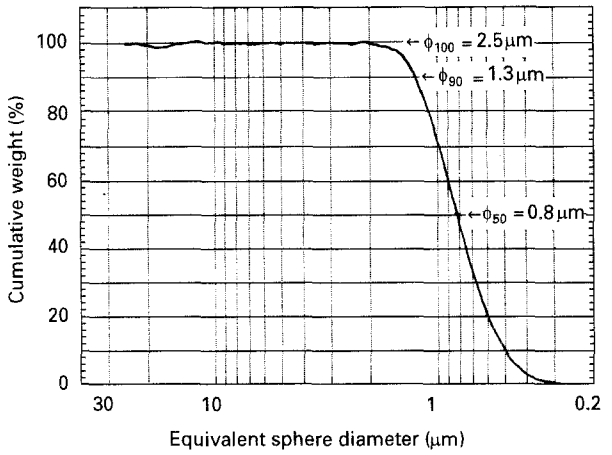

Figure 1 Sedimentation curve for an Ag/Pd powder 70%/30% dispersed by sonication in a water–zonyl mixture.

2. Experimental procedure

Direct observation of the powders was made by scanning electron microscopy (SEM) on a Jeol JSM 840 apparatus, to reveal the shape of the particles, their diameter, Φ_{SEM}, and size distribution. Additional information has been obtained from adsorption measurements by the BET (Brunauer, Emmett, Teller) method on a Monosorb® apparatus from Quantachrome. These measurements lead to the specific developed surface area, S_{BET}, which is itself related to the individual particle sizes. With the hypothesis of monodisperse spherical shaped and bulky crystal particles, the diameter of the particles, Φ_{BET}, is deduced from the surface area, S_{BET}, through the relation

$$\Phi_{BET}(\mu m) = 6/r(g\,cm^{-3})S_{BET}(m^2\,g^{-1}) = 0.55/S_{BET} \quad (1)$$

A good agreement between both values indicates a smooth surface while discrepancy implies a rough one and/or a high polydispersity.

A sedimentation technique was also used which consists in measuring the quantity of particles remaining in suspension as a function of time. This measurement is based on the transmittance of a thin X-ray beam. An example of a sedimentation record (obtained on a micromeritics Sedigraph® 5000 apparatus) is given in Fig. 1. Φ_{50} (or Φ_{90} and Φ_{100}) is the upper diameter of 50% (or 90% or 100%) in mass of the mobile particles remaining in solution. These mobile particles are either individual grains, or agglomerates of several grains which are so strongly bound that they cannot be dispersed by sonication. The agglomeration factor for a given population is defined as follows: the agglomeration factor for 90% of the particles remaining in solution (i.e. after sedimentation of the first 10% mass fraction) is the ratio $Agg_{90} = \Phi_{90}/\Phi_{BET}$.

Finally, the tap density also gives a rough indication about the agglomeration state of a powder: high tap densities correspond to close-packed particles which can only be obtained with non-agglomerated particles.

The thermal behaviour of the powders was analysed by three combined techniques. The thermogravimetric analysis (TGA) consists in measuring the mass losses or increases accompanying various processes. Physical and chemical events are easily detected by differential thermal analysis (DTA) which gives access to thermal balances. Dilatation or contraction of materials can also be studied by thermomechanical analysis (TMA). The measurements were carried out on Shimadzu apparatus: TGA-50H, DTA-50 and TMA-50.

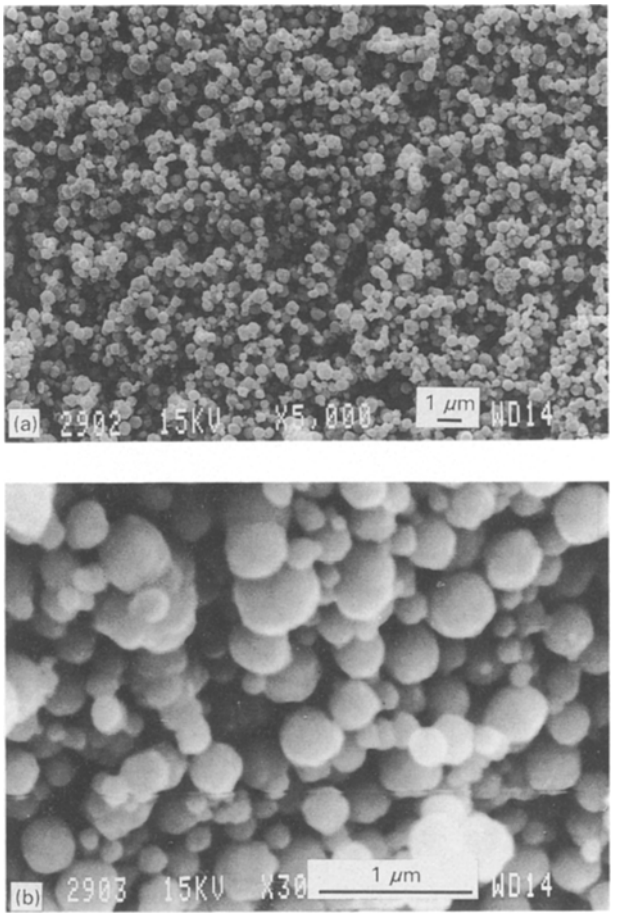

Figure 2 (a, b) Scanning electron micrographs of an Ag–Pd powder.

3. Results and discussion

3.1. Morphology

The powder content is 70/30 or 75/25 Ag/Pd % wt/wt. Examples of SEM images are given in Fig. 2, showing individual spherical shaped particles with a mean diameter of 0.3–0.4 μm. Table I gives the results obtained for a set of powders prepared either at the laboratory or the industrial scale. Values of tap density of 2 or 3 are often rather good values: recently, the tap density has been increased to 5 by adjusting the nature and the quantity of a dispersing additive. The sedimentation results reveal a narrow size distribution, as shown by the proximity of the values Φ_{50} and Φ_{90} for instance. Another estimation of the size distribution of the particles was carried out by analysing a scanning electron micrograph: 125 particles were measured and classified as shown in Fig. 3a (class width 0.08 μm). The sizes vary in the range 0.1–0.5 μm.

TABLE I Characteristics of some Ag/Pd powders

Reference	%Ag	D_t	S_{BET} $m^2 g^{-1}$	Φ_{BET} (μm)	Φ_{50} (μm)	Φ_{90} (μm)	Φ_{100} (μm)	Agg_{50}	Agg_{90}	Agg_{100}
CP348	700	3.2	1.3	0.42	0.7	1.3	5.0	1.7	3.1	11.8
CP349	700	3.1	1.4	0.39	0.7	1.2	4.2	1.9	3.1	10.7
CP395	700	2.8	1.1	0.50	1.0	1.7		1.9	3.4	
CP347	700	2.8	1.4	0.39	0.7	1.2	5.2	1.7	3.1	13.2
CP335	700	2.8	1.4	0.39	1.0	1.5	3.5	2.5	3.8	8.9
2355	700	2.6	1.9	0.29						
CP543	750	3.2	1.2	0.46	0.6	1.1		1.3	2.4	
CP490	750	2.6	1.3	0.42	1.0	1.6	4.0	2.4	3.8	9.5
CP491	750	2.8	1.4	0.39	0.8	1.3	2.0	2.0	3.3	5.1
2356	750	2.4	1.7	0.32	0.8	1.5	3.0	2.5	4.1	9.3

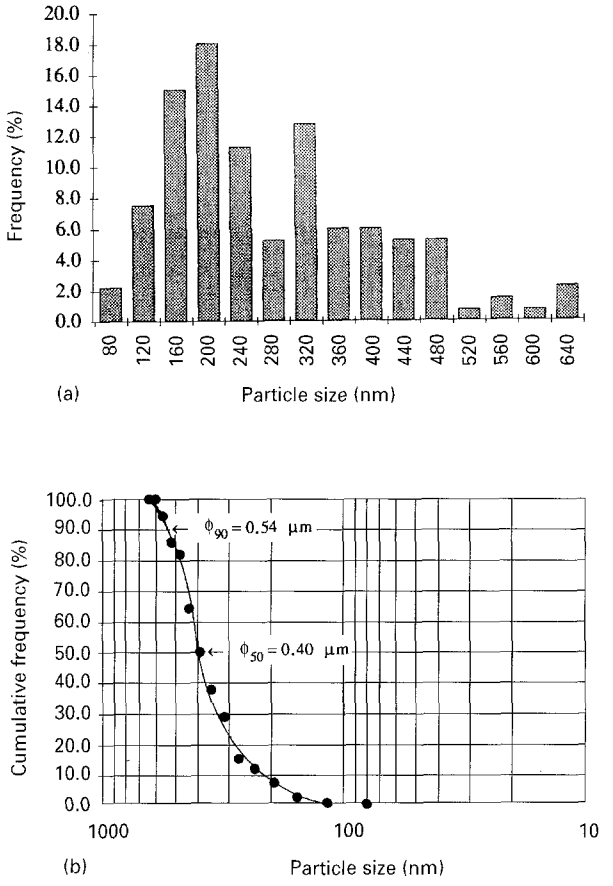

Figure 3 Size distribution of an Ag/Pd powder (CP543, see Table I). (a) Histogram of sizes, (b) cumulative distribution converted into mass for comparison with sedimentation scans. Sample size: 125 particles.

No particle was observed above 0.65 μm or below 0.08 μm. The mean diameter of this sample was 0.28 μm, in coarse agreement with the value deduced from adsorption measurements ($\Phi_{BET} = 0.46$ μm). When converting to mass the data of Fig. 3a, and plotting the cumulated signals (Fig. 3b), a curve comparable to a sedimentation scan can be drawn. The values $\Phi_{50} = 0.40$ and $\Phi_{90} = 0.54$ μm are thus obtained, to be compared to 0.6 and 1.1 μm, respectively, given by sedimentation. Considering that the sedimentation concerns the solvent-separated particles (therefore, possible agglomerates) while the SEM images concern the individual spheres, the results are remarkably close.

From Figs 2 and 3 and the ensemble of the values given in Table I, one can deduce that the powders display very low agglomeration factors: a few units for the whole population; practically no large particle is detected. The agreement between Φ_{BET} and Φ_{SEM} (0.3–0.4 mm) is rather good. When observed by TEM, a few very small particles were detected, but their quantity can be considered negligible.

3.2. Thermal characterization

The key step while preparing conducting layers for MLCCs is the heating of the deposit (a paste made of metal powder dispersed in an organic vehicle, then screenprinted and dried) at 1000 °C in air: during this step, the remaining organic components are burnt out and the powder grains sinter into a metal laydown responsible for the conducting properties. Many other events are known to happen during the process, namely oxidation of palladium, then reduction of the oxide PdO, and dimensional modifications accompanying every phenomenon. All these changes may induce defects in MLCCs, thereby decreasing the electrical performance of the product. For this reason, we have studied the thermal behaviour of the powders and also of the subsequently deposited layers.

The powders were observed by two combined techniques: DTA and TGA, while heating in the temperature range 20–1000 °C in air (heating rate 10 °C min^{-1}). The measurements were carried out on dry powders. Typical recorded curves are shown in Fig. 4a and b for a powder Ag/Pd 70/30.

The TGA signal indicates a mass loss of ca. 0.4% in the range 100–200 °C, then, between 300 and 450 °C, a 2% mass increase followed by a mass loss up to 620 °C. After that the mass is quite stable. The initial mass loss corresponds to the elimination of water traces and firing of organic residues (see the small peak in the DTA curve at 187 °C and discussion below). The main phenomenon (300–620 °C) is typical for the oxidation of palladium followed by the reduction of PdO into palladium as described previously [3, 7, 10]: the difference between the baselines at 200–300 °C and above 620 °C is assigned to a partial oxidation of palladium in the initial powder, whose composition is then deduced (PdO 5%, Pd 25%, Ag 70% wt/wt).

The DTA signal is more complex: the small exothermic peak at 187 °C corresponds to the combustion of

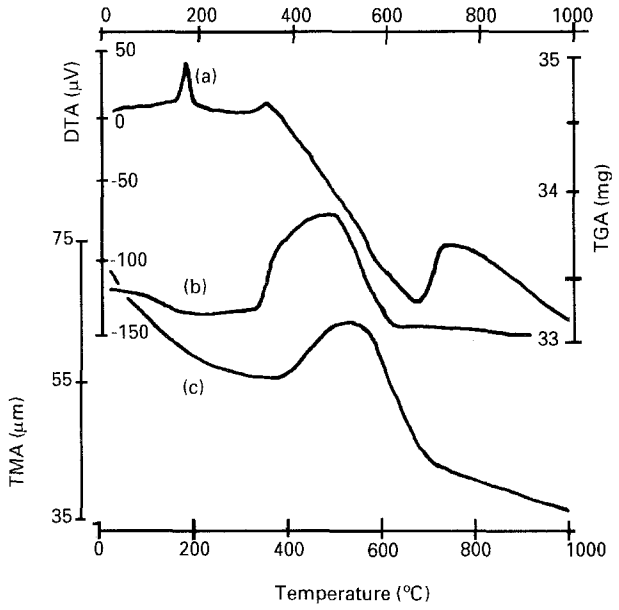

Figure 4 Thermal analysis curves of an Ag/Pd powder 70/30 at the rate 10 °C min^{-1} from 20–1000 °C. (a) TDA on powder, reference alumina. (b) TGA on powder, initial mass 33.41 mg. (c) TMA on powder deposit (see text), reference alumina.

organic residues, in coincidence with the end of the initial mass loss on the TGA curve. The oxide formation after 320 °C is an exothermic process responsible for the beginning of a peak observed at ca. 340 °C [11]; this peak is then rapidly dominated by the opposite tendency of an important endothermic process extending over a wide temperature range. The baseline drift above 700 °C indicates that in the range 340–1000 °C, two endothermic processes occur. One of them clearly corresponds to PdO reduction observed on the TGA curve and finished at 620 °C. The other is a superimposed effect of particle sintering and Pd/Ag interdiffusion as previously described [3]. Actually, because no peak is observed at the melting point of pure silver 960 °C, the DTA curve demonstrates that alloying has been achieved before reaching this temperature. Separate experiments carried out on a powder (CP 543) heated at 300 °C for 24 h indicate that some sintering already occurs at this temperature while no alloying is observed under these circumstances (X-ray diffraction observation).

TMA measurements were performed on powder deposits prepared as follows: an ink (powder + organic binder) was printed on to a ceramic layer and then dried at 100 °C. The TMA curve indicates a progressive shrinkage of the sample up to ca. 400 °C, corresponding to the elimination of remaining water and organic residues; the palladium oxidation–reduction process was also observed through an expansion-shrinkage behaviour, although shifted in temperature. This T-shift is assigned to the very different experimental conditions between the pure metal powder (TGA and DTA) and the deposited layer (TMA). A negative drift of the TMA signal is due to sintering, providing a thining down which is finished at ca. 900 °C. The overall thermo-mechanical variations are low, thus warranting a good compatibility between the metal laydown and its ceramic support.

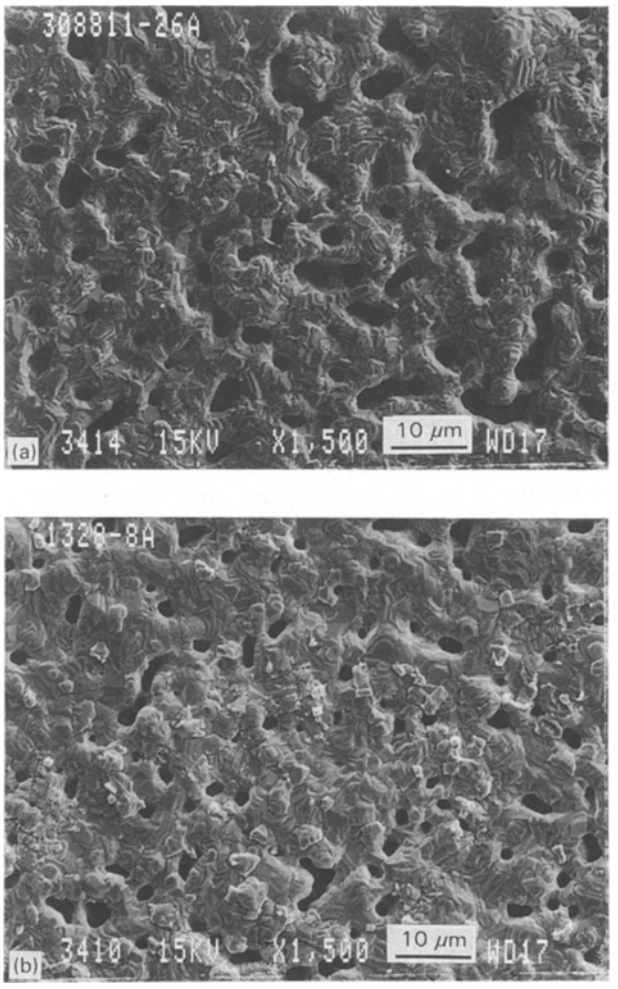

Figure 5 Scanning electron micrographs of Ag/Pd laydowns. (a) Ag/Pd 70/30, mean thickness 1.8 μm, $\rho = 29.0$ μΩ cm. (b) Ag/Pd 75/25, mean thickness 2.1 μm, $\rho = 15.6$ μΩ cm.

3.3. Characterization of the metal laydown

For economic reasons, the metal deposits in MLCCs are required to be as thin as possible while being highly conducting: the highest conductivity is obtained with bulky layers.

Because these powders are intended to be used in multilayer capacitors, they have been tested under the conditions used for this peculiar application, i.e. after deposition on a ceramic substrate (see above) and then firing at 1000 °C in air. Such deposits have been analysed by several techniques.

Typical scanning electron micrographs are shown in Fig. 5 for layers of ca. 2 μm thickness deposited from previous powders (See Table I). In these laydowns, the individual structure of the particles has disappeared, thus providing a quasi-continuous metal film in which only a few voids remain.

The resistivity of the same samples was measured: values of 29.0 and 15.6 μΩ cm were obtained. On the basis of literature data [12], the resistivity of bulk Ag/Pd alloys has been estimated to 15.5 and 12.7 μΩ cm, respectively, for alloy compositions 70/30 and 75/25: the conductivity of the laydowns made from powders appears to be close to these intrisic values.

4. Conclusion

The powders studied here have been shown to be made of submicronic spherical shaped particles displaying a narrow size distribution and very little agglomeration. Such morphological characteristics make them good candidates for being used in the wet-stack process. Indeed, in the printing step of the process, the spherical shape and homogeneous size provide optimization for conductive laydowns: the spherical shape induces a high dispersibility in the paste, favours dense arrangements of the grains and ensures a high reactivity for sintering at the sphere contacts. Then, under heating, sintering is favoured in order to form an almost continuous metal layer. Although the particles are not initially alloyed, interdiffusion is easily achieved so that no melting is observed below 1000 °C: this is due to the extreme proximity of the silver and palladium phases because both metals are present in every particle in a core–shell structure [9]. Therefore, these powders appear well adapted to the wet-stack MLCC manufacturing applications.

Acknowledgements

This work was financially supported by ADEME (Agence De l'Environnement et de la Maîtrise de l'Energie). The authors thank R. Laval, CEETAM, Orsay, for SEM observations.

References

1. G. G. FERRIER, A. R. BERZINS and N. M. DAVEY, *Platinum Metals Rev.* **29** (1985) 175.
2. L. C. HOFFMANN. *Adv. Ceram.* **19** (1986) 71.
3. K. NAGASHIMA, T. HIMEDA and A. KATO, *J. Mater. Sci.* **26** (1991) 2477.
4. M. H. LA BRANCHE, J. G. PEPIN and W. BORLAND, in "Proceedings of the ASM Thick film Conference", Atlanta, GA June 1988.
5. J. G. PEPIN, *J. Mater. Sci. Mater. Electron.* **2** (1991) 34.
6. S. F. WANG and W. HUEBNER, *J. Am. Ceram. Soc.* **74** (1991) 1349.
7. S. F. WANG, W. HUEBNER and C. Y. WANG, *ibid.* **75** (1992) 2232.
8. D. L. THIEBAULT, in "Precious Metals", edited by A. K. Mehta and R. M. Nadkarni (International Metal Precious Institute and Nielson, Austin, Texas, 1992) p. 257.
9. F. YALA, C. HAUT, C. SEVERAC, C. GRATTEPAIN, E. DELARUE and M. O. DELCOURT, *J. Mater. Sci.* **30** (1995) in press.
10. S. R. COLE Jr, *J. Am. Ceram. Soc.* **68** (1985) C106.
11. J. G. PEPIN, W. BORLAND, P. O'CALLAGHAN and R. J. YOUNG, *ibid.* **72** (1989) 2287.
12. B. SVENSSON, *Annal. Physik.* **5** (1932) 699.

Received 23 February
and accepted 27 July 1994